Clays and Clay Minerals, Vol. 46, No. 1, 69–78, 1998.

LATE-STAGE DIAGENESIS OF ILLITIC CLAY MINERALS AS SEEN BY DECOMPOSITION OF X-RAY DIFFRACTION PATTERNS: CONTRASTED BEHAVIORS OF SEDIMENTARY BASINS WITH DIFFERENT BURIAL HISTORIES

BRUNO LANSON,[1] BRUCE VELDE[2] AND ALAIN MEUNIER[3]

[1] Environmental Geochemistry Group, LGIT IRIGM, University of Grenoble and CNRS, BP 53-38041, Grenoble Cedex 9, France

[2] Laboratoire de Géologie, CNRS, Ecole Normale Supérieure, 24 rue Lhomond, 75231 Paris Cedex 05, France

[3] Laboratoire de Pétrologie des Altérations Hydrothermales, CNRS, Université de Poitiers, 40 av. Recteur Pineau, 86022 Poitiers Cedex, France

Abstract—The smectite-to-illite diagenetic transformation has been documented in 5 different sedimentary basins using X-ray diffraction (XRD). Intermediate reaction products coexisting because of the effect of kinetics on this reaction have been characterized using decomposition of XRD patterns and comparison with calculated patterns. The nature and relative abundances of the various subpopulations of particles are shown to vary as a function of the geothermal gradient and of the age of the sediment. In all sedimentary basins that experienced a low steady geothermal gradient the physico-chemical characteristics (coherent scattering domain size [CSDS], junction probabilities) of intermediate mixed-layered illite–smectites (I–S) are similar. However, both the relative abundance and the crystallinity of the end-member illite increase as a function of the age of the sediment.

In basins that have experienced a higher geothermal gradient, the CSDS of the I–S subpopulation is higher for a given illite content, indicating a slightly different reaction pathway. This difference in the characteristics (peak position and width) of elementary peaks may be used to infer the presence of such a high geothermal gradient when no other data are conclusive. In this case the growth of the illite end-member is favored over the growth of intermediate I–S phases even in young basins. Illitic phases formed from the alteration of kaolin minerals exhibit characteristics similar to the reaction products of the smectite-to-illite diagenetic transformation in the case of a high geothermal gradient. In contrast with what is observed in shale diagenesis, the characteristics of the illitic subpopulations describe a continuum with absolutely no gap in between subpopulations. In sandstone reservoirs, the various subpopulations crystallize simultaneously from a kaolin precursor. As a consequence, no kinship is expected between the various subpopulations.

Key Words—Clay Minerals, Decomposition, Diagenesis, Illite, Illite–Smectite, Mixed Layering, X-ray Powder Diffraction.

INTRODUCTION

Diagenetic evolution of clay minerals has been extensively described for over 20 years by many authors. Smectite illitization, especially, is shown to occur almost systematically in argillaceous diagenetic series (Burst 1969; Perry and Hower 1970; Hower et al. 1976; Boles and Franks 1979; Środoń 1979, 1984; Velde et al. 1986; Glasmann et al 1989; McCarty and Thompson 1991; Velde and Vasseur 1992; Pollastro 1993; Lindgreen 1994; Hillier et al. 1995; Varajao and Meunier 1995). XRD has been the essential tool used to identify and characterize the reaction sequence:

Smectite ⇒ randomly interstratified illite–smectite mixed layer (I–S) ⇒ ordered I–S ⇒ illite [1]

Additionally, an apparent kinetic effect has been shown for this transformation by comparing clay mineral evolution in wells of different ages (Lahann 1980; Środoń and Eberl 1984; Velde 1985; Velde et al. 1986; Jennings and Thompson 1986; Freed and Peacor 1989; Velde and Vasseur 1992; Pollastro 1993). This apparent kinetic effect is also demonstrated from the comparison of the maturation of organic material to reaction progress of I–S products in the same rock samples (Francu et al. 1989; Velde and Espitalié 1989; Pollastro 1993; Hillier et al. 1995).

In spite of this apparent kinetic effect, the driving force for the smectite-to-illite conversion is likely to be unique, at least for the end of the illitization reaction, and related to the minimization of free energy for the I–S particle population (Eberl and Środoń 1988; Lanson and Champion 1991). This minimization first implies the progressive illitization of I–S and, ultimately, the improvement of illite crystallinity. However, because of the kinetic effect the precursor smectitic I–S will evolve as a function of the time–temperature conditions experienced by the sediments. As a consequence, it is especially important to precisely describe intermediate I–S phases because they are likely characteristic of different reaction pathways.

Table 1. Geographic, stratigraphic and bibliographic information about the samples described in this study.

Location	References	Well	Samples	Stratigraphy	Present depth (m)
Illinois basin (USA)	Gharrabi and Velde 1995	#66	27	Carboniferous–Cambrian	130–2652
		#13	20	Carboniferous–Devonian	487–1615
		New Albany group	16	Devono-Mississipian	146–1475
Paris basin (F)	Lanson 1990;	M	66	Portlandian–Keuper	1275–3119
	Lanson and Champion 1991;	D	83	Cretaceous–Permo-Trias	800–3572
	Lanson and Besson 1992;	C	62	Lias–Stephanian	60–2130
	Lanson, unpublished data	L	46	Maastrichtian–Autunian	105–3604
		Cr	19	Senonien–Permien	385–3090
Gulf Coast (USA)	Matthews, unpublished data; Lanson 1990;	G	40	Miocene	1528–5300
	Velde and Vasseur 1992	Mustang Island	45	Oligocene (Frio/Vicksburg)	958–5233
Niger delta (Nigeria)	Velde et al. 1986		22	Lower Cretaceous	630–2454
Rotliegend sandstone reservoir	Lanson et al. 1995, 1996	1	7	Lower Permian	2976–2991
		2	12	Lower Permian	3320–3495
Broad Fourteens basin (NL)		3	17	Lower Permian	4230–4485
		4	15	Lower Permian	2479–2546
		5	16	Lower Permian	2880–2970
		6	9	Lower Permian	2893–2948
Roliegend sandstone reservoir	Lanson, unpublished data	7	20	Lower Permian	1889–1938
		8	17	Lower Permian	2253–2270
On shore (NL)		9	13	Lower Permian	1512–1520
		10	13	Lower Permian	2267–2278
		11	25	Lower Permian	2570–2668
Sergipe-Alagoas basin (BZ)	Varajao and Meunier 1995	FU-1	25	Lower Cretaceous	513–2457
		FU-25	12	Lower Cretaceous	993–1773
		CSMC	18	Lower Cretaceous	1095–2631
		SMC	18	Lower Cretaceous	1245–2732
		BSM	14	Lower Cretaceous	2460–3325
		Total	697		

Using the decomposition procedure for the processing of XRD profiles, the present paper describes the structural characteristics of the various subpopulations forming illitic clay assemblages. Shale samples from 5 different illitization sequences are studied in the light of the diagenetic histories of the sediments. These samples are then compared to illitic products formed directly from the alteration of kaolin-group minerals in a reservoir sandstone.

EXPERIMENTAL

Samples

Most of the 700 samples (from about 30 deep wells) used for this study have been described previously and extensively by various authors and their significance in terms of diagenetic conditions is also described in detail (Velde et al. 1986; Lanson 1990; Lanson and Champion 1991; Lanson and Besson 1992; Velde and Vasseur 1992; Gharrabi and Velde 1995; Varajao and Meunier 1995; Lanson et al. 1996). References and stratigraphy of these sequences are given in Table 1. Generally, samples from the Illinois basin represent the typical evolution of I–S under low-temperature conditions over a long period of time (Gharrabi and Velde 1995). Both clay-mineral and organic matter evolution indicate a progressive burial with a constant thermal gradient of 30 °C/km from deposition time to the Tertiary (50 Ma) followed by the erosion of about 1500 m of overburden over the 50–2 Ma time span. The burial history of the Paris basin looks very similar to that of the Illinois basin, with a progressive burial (constant thermal gradient of 35 °C/km) followed by erosion of about 600 m of overburden in the center of the basin (Velde and Vasseur 1992; Gharrabi and Velde 1995). It should be noted that 4 of the 5 wells sampled are located in the center of the basin where the erosion is minimal. The fifth well is located in the eastern part of the basin where most of the late Cretaceous–early Tertiary section has been removed. A similar progressive burial with a constant low thermal gradient (33 °C/km) has been described for Gulf Coast sequences (Velde and Vasseur 1992). The main difference in the Gulf Coast versus the Illinois and Paris basins is the younger age (Oligocene) of the Gulf Coast sediments. Characteristic XRD patterns from the Paris basin and from the Gulf Coast area are shown in Figure 1.

In the Niger delta, the burial history is intermediate between those observed for the Paris basin and the Gulf Coast area. However, the Niger delta has a much higher geothermal gradient (about 100 °C/km) than in the other study areas (Velde et al. 1986). The burial and thermal history of the fifth area, the Sergipe–Alagoas basin, is unresolved as there is no agreement on the evolution of clay minerals and the maturation of

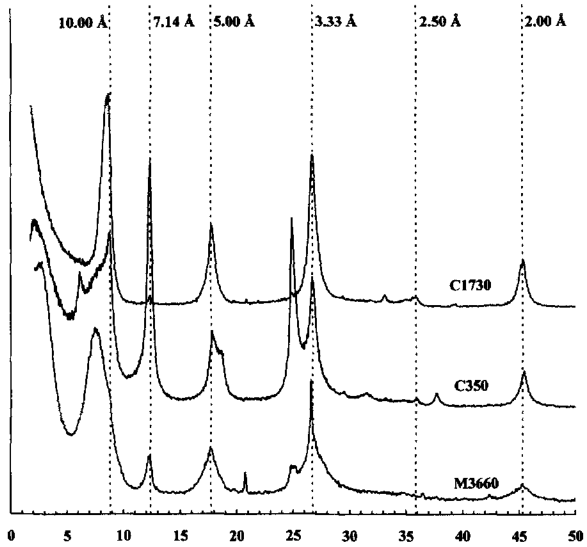

Figure 1. Characteristic XRD patterns of air-dried samples from the Gulf Coast area (M3660, Mustang Island 3660 m) and from the Paris basin (C350 and C1730, Well C 350 and 1730 m, respectively). References to these wells are in Table 1. Size fraction is less than 2.0 μm.

organic matter obtained from vitrinite reflectance data (Varajao and Meunier 1996). The sediments from this area are similar in age to those from the Niger delta area, both areas being symmetrically distributed on both sides of the southern Atlantic Ocean. Combined, the samples from our study represent the evolution of I–S in shales from a variety of burial histories. To ensure similar lithology, all samples, except for a few wells from the Paris basin, were hand-picked shale fragments.

The last area sampled, the Rotliegend sandstone reservoir in the Netherlands (both onshore and offshore), represents a different pathway for the formation of illitic phases (illite and illitic I–S). The permeability of the Rotliegend sandstone reservoir is much higher (up to several hundreds mD) than that of the shales from the other 5 areas. Further, the illitic material does not result from a steady smectite-to-illite evolution with increasing depth but from the sudden illitization of kaolin-group minerals in response to an influx of K-rich brines into the reservoir (Lanson et al. 1995, 1996). Even though there was a significant increase of the heat flow during the Kimmerian orogeny, the geothermal gradient was quite low during the whole burial history as maximum temperatures range from ~110 °C at 3000 m to ~165 °C at 5000 m (estimated maximum burial depth; Lanson et al 1996).

Methods

All samples were studied by XRD on both air-dried (AD) and ethylene glycol- (EG) or glycerol- (GLY) solvated oriented preparations of similar size fractions (usually <2 μm, and <5 μm for the samples from the Rotliegend sandstone reservoir). Results reported here have all been obtained on the 14–10 Å band (Lanson and Velde 1992) observed on AD patterns and related to I–S and illite phases. However, for any series of samples several EG, or GLY, patterns have been processed with the decomposition routine to check the consistency of the decomposition performed on the AD pattern (Lanson 1997). Details on the various experimental settings used to record XRD patterns are given by the respective authors. All experimental XRD patterns recorded on AD samples were fitted with several elementary curves assumed to represent the respective contributions from the various subpopulations of particles to the total profile using a unique calculation code (DECOMPXR; Lanson 1990, 1997). For all samples, the acceptable fits (Lanson 1997) were obtained using at least 1 elementary peak for the ordered I–S (R1) and 1 for illite. Most often (all samples except those from the Gulf Coast area) the illite contribution was fitted with 2 elementary peaks associated with the poorly crystallized (PCI) and well-crystallized (WCI) end members of the illite particle population (Lanson and Meunier 1995; Lanson 1997). If necessary, additional elementary peaks were introduced to account for the contributions of randomly interstratified I–S (R0) and chlorite. Except for the usual parameters such as peak position or width (full width at half maximum intensity [FWHM]) an additional parameter was derived from these fits for the present study. The I–S over illite ratio parameter is the ratio of the surface areas of I–S peaks (R1 plus possibly R0) over the surface areas of illite (PCI plus WCI). The surface area is calculated for any elementary peak from adjusted FWHM and intensity.

EXPERIMENTAL RESULTS

Low Steady Geothermal Gradient (Illinois Basin–Paris Basin–Gulf Coast Area)

Within the 3 basins with similar low, constant geothermal gradients (30–35 °C/km) the abundance of ordered I–S can be related to the age of the sediments. The I–S subpopulation is more abundant in the younger sediments of the Gulf Coast area and in the shallowest samples from the Paris basin (Figure 1). In older sediments, the 10-Å band is dominated by the contributions of illite (PCI and WCI) over I–S with a maximum at 10 Å showing an asymmetry on the low-angle side. In spite of contrasting relative abundances, the characteristics of the I–S are very similar for the 3 areas. The FWHM versus peak position trends obtained for all samples from the 3 areas may be superimposed to the one obtained for the Illinois basin, which may be considered as typical of the I–S mineral transformation under low temperature for very long

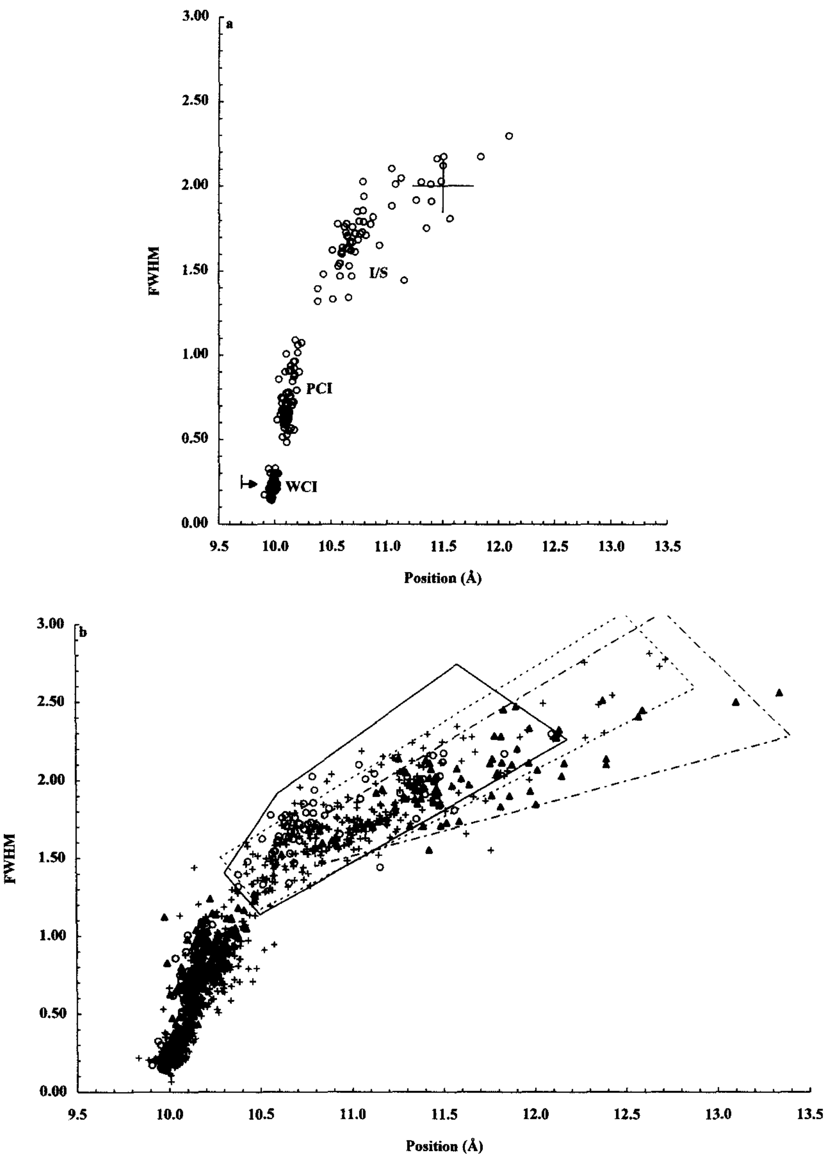

Figure 2. a) FWHM plotted as a function of position for the various elementary peaks fitted on experimental diffraction profiles obtained on samples from the Illinois basin (air-dried state). The error bars are those given by Lanson (1997). WCI, PCI and I–S refer respectively to the well-crystallized illite, poorly crystallized illite and illite–smectite mixed-layer subpopulations associated to the various elementary peaks (Lanson and Meunier 1995). b) Comparison of the FWHM-position trends obtained for WCI, PCI and I–S elementary peaks fitted on experimental XRD profiles from the Illinois basin (open circles), the Paris basin (crosses) and the Gulf Coast area (solid triangles). The solid line defines the I–S domain for the Illinois basin samples. The regular and irregular dashed lines define the I–S domains for the Paris basin and Gulf Coast area samples, respectively.

periods of time (Figures 2a and b). However, one may note that the FWHM of I–S elementary peaks from the Gulf Coast area is slightly lower for a given position, indicating a slightly improved crystallinity. The uniqueness of the global trend indicates that for a given composition both the stacking sequences (junction probabilities) and the average CSDS are similar in all 3 study areas. Additionally, one may note (Figure 2b) that the I–S domain is more and more limited on the high-smectite side as the age of the basin increases; the I–S domain is much smaller for the Illinois basin than for the Gulf Coast area. Simultaneously, this domain shifts gradually to include more illitic, better crystallized I–S. Except for the relative contributions of the various subpopulations, there is one major difference between the Illinois basin and the Paris basin on the one hand and the Gulf Coast area on the other hand. In the former, the 2 end members of the illite particle population, PCI and WCI, are well expressed and define separated domains (Figures 3a and b). In the younger Gulf Coast sediments, in addition to its relatively lower abundance, the illite particle population is not as well crystallized. For some samples it was impractical to separate the respective contributions of PCI and WCI, and the resulting peak characteristics lie in between the 2 domains (Figure 3c). In any case the global illite domain is much more extended towards high FWHM, and high *d*(001), indicating smaller CSDS.

High Geothermal Gradient
(Niger Delta–Sergipe-Alagoas Basin)

For both series of samples, the characteristics of both I–S and illite peaks are very similar and will be described together. The FWHM versus peak position trend (Figure 4) is different from that of the 3 basins with a constant low geothermal gradient. For a given peak position, the FWHM is lower, indicating a larger CSDS, as the broadening related to interstratification may be considered constant for a given I–S peak position. In addition to this improved crystallinity of I–S, both end members of the illite particle population are well separated to indicate the presence of illite particles with large CSDSs.

Chemically Induced Illitization (Rotliegend Sandstone Reservoir of The Netherlands)

For this series of samples, the FWHM versus peak position trend (Figure 5) is similar to the one obtained for the former 2 basins. However, if the characteristics (composition, junction probabilities and CSDS) of these illitic phases are very similar, there is a major difference among the various subpopulations. There is no apparent limit among the I–S, PCI and WCI domains, even though the same decomposition routine and logical procedure were used to obtain the fits. The characteristics of the illitic phases describe a complete continuum.

Relative Abundances of I–S and Illite Subpopulations

As this has been described qualitatively on Figure 1 for the 3 basins with low constant geothermal gradient, the relative abundance—estimated from the relative surface areas of I–S, PCI, and WCI peaks—of I–S subpopulation versus illite subpopulations is higher when the age of the sediment is lower. This is consistent with the observations of Velde and Lanson (1993; Figure 1). On Figure 6a, the ratio between the surface area of elementary peaks associated with I–S (R0 plus R1) and the surface area of elementary peaks associated with illite (PCI plus WCI) is much higher for Gulf Coast samples than for Illinois basin samples. The behavior of the samples from the Paris basin is intermediate between the previous two, as the shallowest samples from the Paris basin (Tertiary to Late Cretaceous in age) behave roughly as the samples from the Gulf Coast area whereas the deeper samples (Permian to Stephanian in age) behave as the samples from the Illinois basin. This may indicate that kinetics of illite growth is very slow in a basin submitted to a low geothermal gradient. In both Lower Cretaceous basins (Niger delta and Sergipe-Alagoas) the trend is similar to the one observed in older basins. There is an overwhelming presence of illite over I–S (Figure 6b). This is equally true for illitic material crystallized directly from kaolin-group minerals (Rotliegend sandstone reservoir; Figure 6c).

DISCUSSION

From the above observations, it is possible to derive a global scheme for the smectite-to-illite conversion process in sediments. In all examples described in this paper, as well as in most basins studied since Hower and Mowatt (1966), well-crystallized illite is undoubtedly the ultimate product of the smectite-to-illite diagenetic transformation. However, because of an apparent kinetic effect, various subpopulations of particles with different mean characteristics (composition, CSDS, junction probabilities) may coexist (Lanson and Champion 1991). Using decomposition of XRD profiles, it is possible to characterize these coexisting subpopulations. Here I–S, PCI and WCI (Lanson and Meunier 1995) coexist. These subpopulations are representative of various steps during the illitization process. In response to increasing temperature conditions, the physical characteristics of these subpopulations (composition, CSDS) evolve as do their relative proportions. With increasing diagenetic conditions (time and temperature), not only I–S particles become progressively more and more illitic but, in addition, illite crystals grow at the expense of I–S, in agreement with Pollastro (1985). The I–S illitization and illite growth are promoted in contrasting ways as a function of the time-temperature conditions experienced by the sediments.

Illite Subpopulation

In basins which experienced a steady burial with a low geothermal gradient (Figure 7a) WCI is the most favored subpopulation in the oldest sediments as all major pathways (large black arrows) tend to form WCI. With increasing burial, the I–S subpopulation is progressively illitized, part of I–S crystals grow (small light gray arrows) but most of them are dissolved as PCI and WCI particles dominate the assemblage. This results in the presence of a well-expressed WCI subpopulation and, as a consequence, in an increase of the illite mean CSDS (crystallinity). Restriction of the discrete illite domain and its shift towards both lower *d*-values and lower FWHM with increasing burial time (Figure 3)

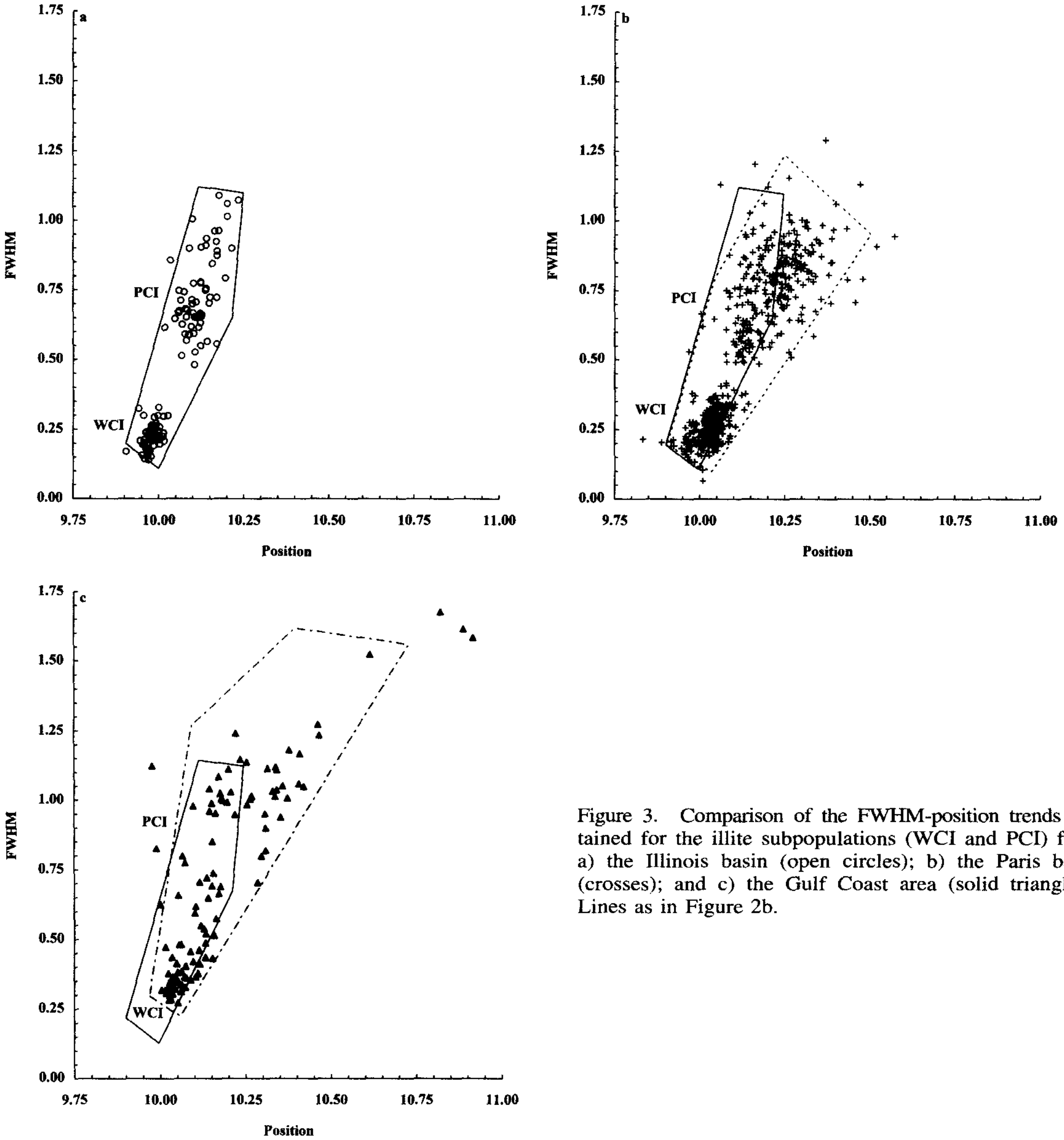

Figure 3. Comparison of the FWHM-position trends obtained for the illite subpopulations (WCI and PCI) from a) the Illinois basin (open circles); b) the Paris basin (crosses); and c) the Gulf Coast area (solid triangles). Lines as in Figure 2b.

is characteristic of this improved illite crystallinity. In the Gulf Coast area, which experienced a similar low constant geothermal gradient but, in contrast, a short and deep burial, the favored subpopulation is the I–S one (Figure 7b), as the growth of illite subpopulation is limited as indicated by the small light gray arrows. However, one may note that the characteristics of this I–S subpopulation are very similar to those observed in the former basins. Even though the end-member illite (PCI, and WCI on a lower extent) is present, its abundance is very low, the formation of discrete illite from I–S crystals being limited, and its crystallinity is low as shown by the unique presence of a PCI peak in the samples from Mustang Island well. This is probably induced by very slow kinetics of the last step of the smectite-to-illite conversion, that is, crystallization of WCI. However, as shown by the results obtained in the Niger delta area, this last step may be thermally enhanced if the geothermal gradient is high enough. This is consistent with the experimental data obtained previously for geothermal (Yau et al. 1987) and nongeothermal recent sediments (Jennings and Thompson 1986). In such cases, the most favored subpopulation is WCI (Figure 7c), all major pathways (large black arrows) tending to form WCI, as it is for long steady burial and low geothermal gradient.

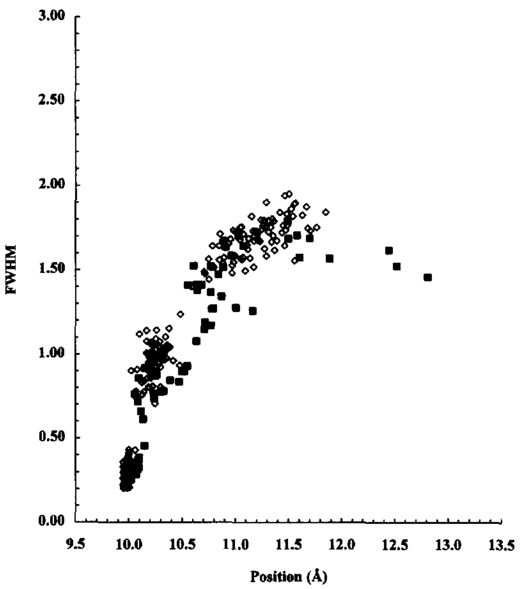

Figure 4. Comparison of the FWHM-position trends obtained for WCI, PCI and I–S elementary peaks fitted on experimental XRD profiles from the Niger delta area (solid squares), and the Sergipe-Alagoas basin (open diamonds).

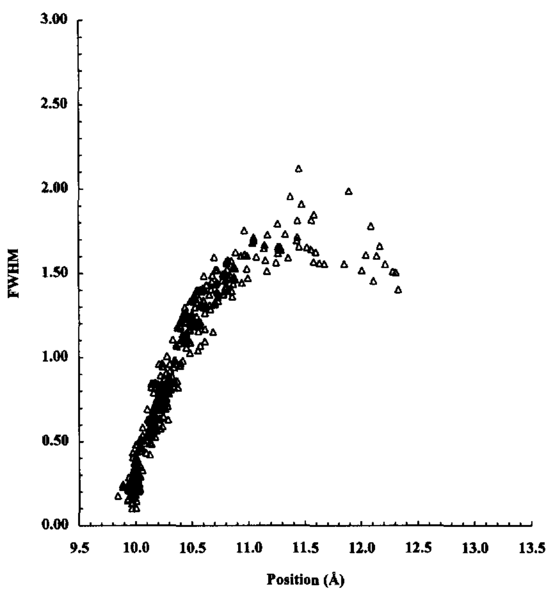

Figure 5. FWHM-position trend obtained for WCI, PCI and I–S elementary peaks fitted on experimental XRD profiles from the Rotliegend sandstone reservoir (open triangles).

Illite–Smectite Subpopulation

The results from the present study show that the characteristics of the intermediate I–S products differ as a function of temperature gradient. The mean CSDS of the I–S subpopulation increases with increasing temperature gradient (Figures 2b, 4 and 5), even though all intermediate reaction products are ordered I–S with comparable compositional ranges. The origin of this influence of the temperature gradient on the physical characteristics of the I–S particle subpopulation is unknown. However, one may note that the CSDS of a crystallite will be higher, for a given composition, if illite and smectite layers, rather than only illite layers, grow on the same initial crystallite. One may also note that a strict layer-by-layer solid-state smectite-to-illite transformation would result in a very low, and constant, CSDS for all intermediate I–S and PCI material as there is no growth of external layers in such a case.

Additionally, from the present data it seems realistic to constrain further hypotheses on the existence of a high geothermal gradient from a FWHM-versus-position plot, which is roughly equivalent to a CSDS-versus-composition plot. For example, in the case of the Sergipe-Alagoas basin it seems reasonable to assume that the very mature, illite-rich I–S may result from as high a gradient as in the corresponding Niger delta. The existence of contrasting intermediate I–S material may also account for the kinetic influence on the smectite illitization and especially on the crystallization of end-member illite. To massively grow well-crystallized I–S crystallites as a first step and to dissolve these large crystals to grow end-member illite as a second step is likely not to be favored energetically.

The 5 sedimentary basins studied document the smectite-to-illite conversion series and consistently show that each subpopulation presents specific characteristics contrasting with the other subpopulations. These subpopulations usually form separated domains and seem to be rather individualized. Moreover, the various subpopulations behave specifically in response to diagenetic conditions, as they have specific crystallochemical characteristics (CSDS, composition) as a function of these conditions and as they are growing or dissolving (Figure 7). In the case of the Broad Fourteens basin, where illitic material precipitates directly from kaolinite, the opposite may be observed. Even though the characteristics of the various subpopulations are similar to those described for high geothermal gradients, the different subpopulations form no clearly defined domains. There is no gap from illitic I–S to WCI. This continuum may be understood from a mechanistic point of view. In the first case, there is a conversion sequence I–S ⇒ PCI ⇒ WCI where each individual subpopulation may retain part of the structural characteristics from their precursors. Conversely, in the latter case the 3 subpopulations crystallize simultaneously. Their characteristics vary as a function of the temperature conditions during the illitization event (Figure 7d), but as no kinship exists between the various subpopulations no inheritance from former intermediate stages is expected.

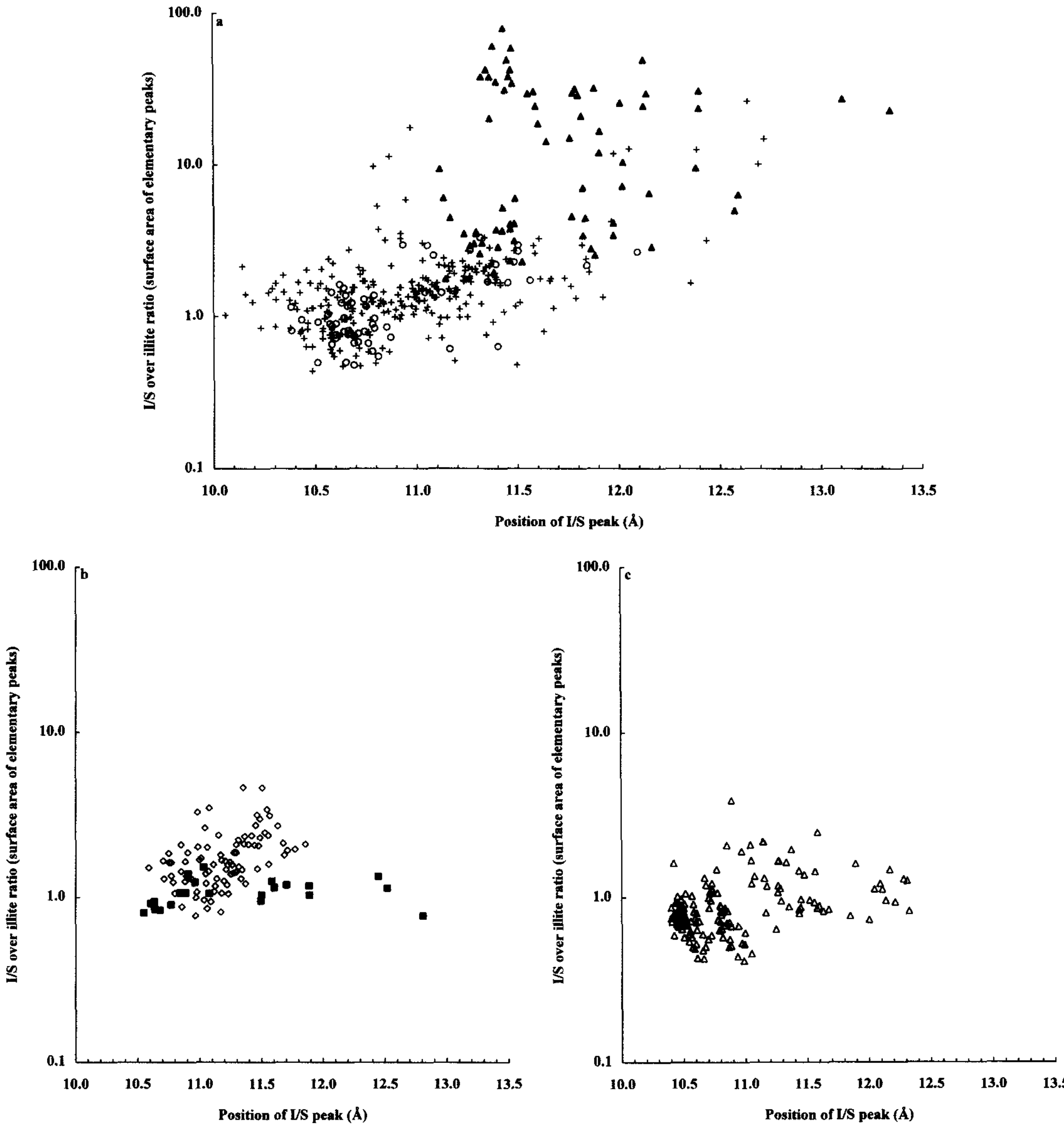

Figure 6. I–S over illite ratio as a function of the illitization progress. The I–S over illite ratio is characterized by the ratio between the surface area of elementary peaks associated with I–S subpopulations (R0 plus R1) and the surface area of elementary peaks associated with illite subpopulations (PCI plus WCI). These surface areas are calculated for any elementary peak from adjusted FWHM and intensity after the decomposition process. The peak position of the I–S (R1) peak is used as an indicator of the illitization progress. a) Comparison between the Illinois basin, the Paris basin and the Gulf Coast area. Symbols as for Figure 2. b) Comparison between the Niger delta area and the Sergipe-Alagoas basin. Symbols as for Figure 4. c) Data from the Rotliegend sandstone reservoir. Symbols as for Figure 5.

CONCLUDING REMARKS

From the experimental data in this study, WCI is undoubtedly the ultimate reaction product for the illitization of both smectitic I–S precursors and kaolin-group minerals. However, the physical characteristics (composition, CSDS) of coexisting crystallite subpopulations (I–S, PCI, WCI), as well as their relative proportions may be representative of time–temperature conditions experienced by the sediments in the case of a progressive smectite-to-illite conversion. The structural characteristics of I–S subpopulation (CSDS and junction probabilities) depend on the geothermal gradient but not on the age of the sediment. This may be used to assume the existence of high geothermal gradient if no other data give conclusive evidence. Additionally, for a given sedimentary age the relative proportions of I–S and illite subpopulations are a function of the thermal gradient, the growth of illite (WCI)

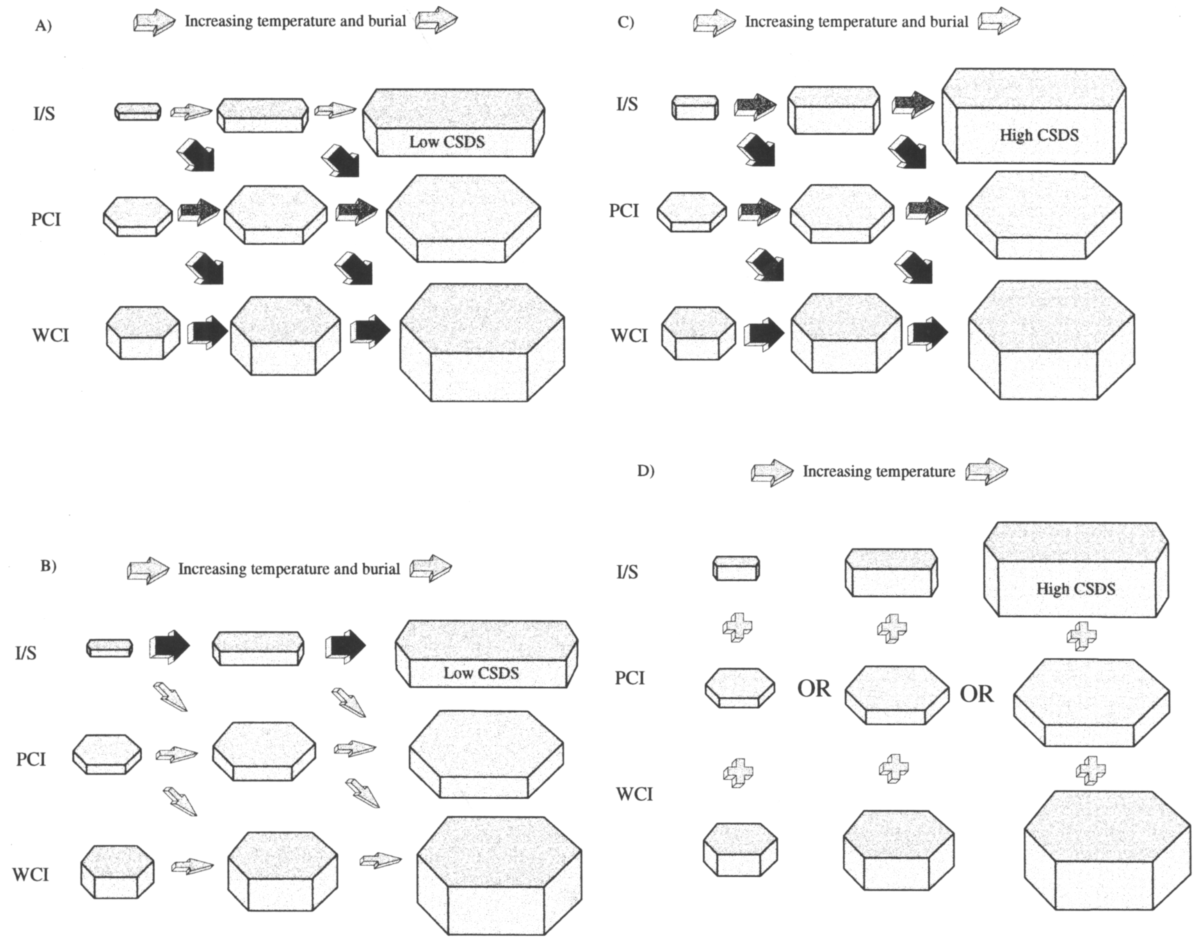

Figure 7. Schematic representation of the I–S to illite reaction pathways as a function of diagenetic conditions. Arrows sizes are indicative of the relative importance of the various transitions. Large black arrows indicate dominant pathways; medium size dark gray arrows indicate intermediate pathways; small light gray arrows indicate secondary pathways. For each subpopulation, the thickness of the schematic particle is indicative of the average CSDS. a) Scheme for a low constant geothermal gradient and a long steady burial (Illinois basin and Paris basin). b) Scheme for a low constant geothermal gradient and a short steady burial (Gulf Coast area). c) Scheme for a high constant geothermal gradient and a short burial (Niger delta area and Sergipe-Alagoas basin). d) Scheme for the illitization of kaolin-group minerals (Rotliegend sandstone reservoir).

being promoted if the gradient is high enough. For a constant low gradient, the kinetics of this growth are very slow. Finally, the absence of a gap, in the proposed FWHM-versus-position plot, from illitic I–S to WCI where illitic material crystallizes directly from kaolin-group minerals could be related to the absence of kinship between the various subpopulations, as I–S is not the precursor for illite in this case. On the contrary, in smectite-to-illite conversion series each subpopulation forms separated domains and seems to be rather individualized.

ACKNOWLEDGMENTS

The authors thank A. Varajao, M. Gharrabi and J. Matthews for using their results. Elf Aquitaine Production, Petrobras, the Illinois State Geological Survey and the Institut Français du Pétrole are thanked for providing the samples. The manuscript was greatly improved by the comments of R. M. Pollastro, R. C. Reynolds, Jr, and Associate Editor J. Środoń.

REFERENCES

Boles JR, Francks GS. 1979. Clay diagenesis in Wilcox sandstones of Southwest Texas: Implications of smectite diagenesis on sandstone cementation. J Sed Petrol 49:55–70.

Burst JF. 1969. Diagenesis of Gulf Coast clayey sediments and its possible relation to petroleum migration. AAPG Bull 53:73–93.

Eberl DD, Środoń J. 1988. Ostwald ripening and interparticle-diffraction effects for illite crystals. Am Mineral 73:1335–1345.

Francu J, Rudinec R, Simanek V. 1989. Hydrocarbon generation zone in the east Slovakian Neogene basin: Model and geochemical evidence. Geol Carpath 40:355–384.

Freed RL, Peacor DR. 1989. Variability in temperature of the smectite/illite reaction in Gulf Coast sediments. Clay Miner 24:171–180.

Gharrabi M, Velde B. 1995 Clay minerals evolution in the Illinois basin and its causes. Clay Miner 30:353–362.
Glasmann JR, Larter S, Briedis NA, Lundegard PD. 1989. Shale diagenesis in the Bergen High area, North Sea. Clays Clay Miner 37:97–112.
Hillier S, Matyas J, Matter A, Vasseur G. 1995. Illite/smectite diagenesis and its variable correlation with vitrinite reflectance in the Pannonian basin. Clays Clay Miner 43:174–183.
Hower J, Eslinger EV, Hower ME, Perry EA. 1976. Mechanism of burial metamorphism of argillaceous sediment: 1. Mineralogical and chemical evidence. Geol Soc Am Bull 87:725–737.
Hower J, Mowatt TC. 1966. The mineralogy of illites and mixed-layer illite/montmorillonites. Am Mineral 51:825–854.
Jennings S., Thompson GR. 1986. Diagenesis of Plio-Pleistocene sediments of the Colorado River delta, southern California. J Sed Petrol 56:89–98.
Lahann RW. 1980. Smectite diagenesis and sandstone cement: The effect of reaction temperature. J Sed Petrol 50: 755–760.
Lanson B. 1990. Mise en évidence des mécanismes de transformation des interstratifiés illite/smectite au cours de la diagenèse [Ph.D. thesis]. Paris, France: Univ. Paris 6–Jussieu. 366 p.
Lanson B. 1997. Decomposition of experimental X-ray diffraction patterns (profile fitting): A convenient way to study clay minerals. Clays Clay Miner 45:132–146.
Lanson B, Beaufort D, Berger G, Baradat J, Lacharpagne JC. 1996. Late-stage diagenesis of clay minerals in porous rocks: Lower Permian Rotliegendes reservoir off-shore of The Netherlands. J Sed Res 66:501–518.
Lanson B, Beaufort D, Berger G, Petit S, Lacharpagne JC. 1995. Evolution de la structure cristallographique des minéraux argileux dans le réservoir gréseux Rotliegend des Pays-Bas: Bull Cent Rech EAP 19:243–265.
Lanson B, Besson G. 1992. Characterization of the end of smectite-to-illite transformation: Decomposition of X-ray patterns. Clays Clay Miner 40:40–52.
Lanson B, Champion D. 1991. The I–S-to-illite reaction in the late stage diagenesis. Am J Sci 291:473–506.
Lanson B, Meunier A. 1995. La transformation des interstratifiés ordonnés ($S \geq 1$) illite/smectite en illite dans les séries diagénétiques: État des connaissances et perspectives. Bull Cent Rech EAP 19:149–165.
Lanson B, Velde B. 1992. Decomposition of X-ray diffraction patterns: A convenient way to describe complex diagenetic smectite-to-illite evolution. Clays Clay Miner 40:629–643.
Lindgreen H. 1994. Ammonium fixation during illite-smectite diagenesis in Upper Jurassic shale, North Sea. Clay Miner 29:527–537.
McCarty D. K., Thompson, GR. 1991. Burial diagenesis in two Montana Tertiary basins. Clays Clay Miner 39:293–305.
Perry EA, Hower J. 1970. Burial diagenesis in Gulf Coast pelitic sediments. Clays Clay Miner 18:165–177.
Pollastro RM. 1985. Mineralogical and morphological evidence for the formation of illite at the expense of illite/smectite. Clays Clay Miner 33:265–274.
Pollastro RM. 1993. Considerations and applications of the illite/smectite geothermometer in hydrocarbon-bearing rocks of Miocene to Mississipian age. Clays Clay Miner 41:119–133.
Środoń J. 1979. Correlation between coal and clay diagenesis in the Carboniferous of the upper Silesian coal basin. In: Mortland MM, Farmer VC, editors. Proc Int Clay Conf; 1978; Oxford, UK. Amsterdam: Elsevier. p 251–260.
Środoń J. 1984. Mixed-layer illite-smectite in low-temperature diagenesis: Data from the Miocene of the Carpathian foredeep. Clay Miner 19:205–215.
Środoń J, Eberl DD. 1984. Illite. In: Bailey SW, editor. Rev Mineral 13, Micas. Washington, DC: Miner Soc Am. p 495–544.
Varajao A., Meunier A. 1995. Particle morphological evolution during the conversion of I–S to illite in lower cretaceous shales from Sergipe-Alagoas basin, Brazil. Clays Clay Miner 43:14–28.
Varajao A., Meunier A. 1996. Burial and thermal conditions of diagenesis in the lower Cretaceous Barra de Itiuba formation, Sergipe-Alagoas basin, Brazil. Bull Soc Geol Fr 167:597–607.
Velde B. 1985. Clays minerals: A physico-chemical explanation of their occurence. Developments in Sedimentology 40. Amsterdam: Elsevier. 427 p.
Velde B, Espitalié J. 1989. Comparison of kerogen maturation and illite/smectite composition in diagenesis. J Petrol Geol 12:103–110.
Velde B, Lanson B. 1993. Comparison of I–S transformation and maturity of organic matter at elevated temperatures. Clays Clay Miner 41:178–183.
Velde B, Suzuki T, Nicot E. 1986. Pressure–Temperature–Composition of illite/smectite mixed-layer minerals: Niger delta mudstones and other examples: Clays Clay Miner 34: 435–441.
Velde B, Vasseur G. 1992. A kinetic model of the smectite-to-illite transformation based on diagenetic mineral series. Am Mineral 77:967–976.
Yau YC, Peacor DR, McDowell SD. 1987. Smectite to illite reactions in Salton Sea shales: A transmission and analytical electron microscope study. J Sed Petrol 57:335–342.

(*Received 9 December 1996; accepted 10 May 1997; Ms. 2840*)